Palpation Localization of Radial Artery Based on 3-Dimensional Convolutional Neural Networks

Qiliang Chen
Guangzhou University of Chinese Medicine
Yulin Huang
Jihua Laboratory https://orcid.org/0000-0003-4476-3969
JingJing Luo (luojingjing@fudan.edu.cn)
Jihua Laboratory https://orcid.org/0000-0002-3222-1276
Jiacheng Yang
Jihua Laboratory
Hong Lu
Fudan University
Zhongzhi Ji
Jihua Laboratory
Xing Zhu
Jihua Laboratory

Research

Keywords: 3D CNN, palpation localization, temporal convolution, video analysis, Traditional Chinese Medicine

Posted Date: October 18th, 2021

DOI: https://doi.org/10.21203/rs.3.rs-965158/v1

Palpation Localization of Radial Artery Based on 3-Dimensional Convolutional Neural Networks

Qiliang Chen[2], Yulin Huang[1], Jingjing Luo[1,3*], Jiacheng Yang[1], Hong Lu[4], Zhongzhi Ji[1] and Xing Zhu[1]

[1*]Jihua Laboratory, Foshan, 528200, China.
[2]School of Basic Medicine,Guangzhou University of Chinese Medicine, Guangzhou, 510006, China.
[3]Academy for Engineering and Technology,Fudan University, Shanghai, 210043, China.
[4]School of Computer Science,Fudan University, Shanghai, 210043, China.

*Corresponding author(s). E-mail(s): luojingjing@fudan.edu.cn;
Contributing authors: chenqiliang@gzucm.edu.cn;
huangyl@jihualab.ac.cn; Yangjc@jihualab.ac.cn;
honglu@fudan.edu.cn; jizz@jihualab.ac.cn;
zhuxing@jihualab.ac.cn;

Abstract

Palpation localization is essential for detecting physiological parameters of the radial artery for pulse diagnosis of Traditional Chinese Medicine (TCM). Detecting signal or applying pressure at the wrong location can seriously affect the measurement of pulse waves and result in misdiagnosis. In this paper, we propose an effective and high accuracy regression model using 3-dimensional convolution neural networks (CNN) processing near-infrared picture sequences to locate radial artery upon radius at the wrist. Comparing with early studies using 2-dimensional models, 3D CNN introduces temporal features with the third dimension to leverage pulsation rhythms. The model had achieved superior performance accuracy as 0.87 within 50 pixels at picture resolution of 2048*1088. Model visualization shows that the additional dimension of the temporal convolution highlights dynamic

changes within image sequences. This study presents the great potential of our constructed model to be applied in real wrist palpation location scenarios to bring the key convenience for pulse diagnosis.

Keywords: 3D CNN, palpation localization, temporal convolution, video analysis, Traditional Chinese Medicine

1 Introduction

Radial artery pulse diagnosis is an indispensable part of the principle 4-methods of diagnosis in Traditional Chinese Medicine (TCM) [1, 2]. It provides with rich physiological information for health evaluation of patients [3], and is regarded as an important tool in non-invasive diagnostic practice [4]. However, the localization of radial artery pulse, divided into 'Cun'(Inch), 'Guan/Gwan'(Bar), and 'Chi'(Cubit) in TCM [5], relies heavily on the doctor's personal experience currently. This has disadvantages of low efficiency or poor reproducibility [6]. Techniques for accurately, automatically and efficiently locating these three important radial pulse positions can make great contributions for modernization of TCM diagnosis.

Several advanced methods have been used to objectively locate radial artery. One example is to use tactile sense or pressure sensor array[7, 8], but it suffers from low positioning accuracy [9] which relies on the sizes and conformity of sensors [10, 11]. Another study performs non-contact image detection, locating radial artery using thermal imagery [3]. This approach prevents direct contact, however, it depends on the sensitivity of an infrared thermal imaging equipment. Individual variations in the shape of the wrist can also cause irreducible deviations. This paper proposes video location method based on deep learning models, hoping to reduce installation cost while improve location accuracy and repeatability.

Video analysis for localization has been increasingly used to detect position of the monitored object. Related studies include finding object's boundaries [12], detecting stellar position[13], as well as locating human position in complex real-life scene[14]. For medical applications, videos are also used for non-contact monitoring of vital signs[15], monitoring of blood perfusion in free flaps [16], and detection of muscle tension dystonia [17] *etc.*. Contraction and relaxation of the heart's ventricles produce rhythmic circulation changes, which are reflected in such blood volume waveform. In fact, "Guan" of wrist pulse positions has the most obvious periodic beating signal, and studies have shown prominent periodic pulsation signals detected around "Guan" in videos [18, 19]. We propose for the first time to use video analysis combined with vital signal to directly locate "Guan" TCM pulse positions of the radial artery.

In this study we evaluate deep learning models for video analysis in locating the position of the radial artery. Convolution neural networks (CNN) is usually applied to automatically and adaptively detect spatial hierarchies of features

[20] and has already been widely used in the medical field in recent years [21]. Our earlier study has achieved advanced accuracy by using 2-dimensional CNN model with image resolution of 1024*544 [19]. However, this resolution is relatively low, and the 2D CNN method extracts information from a single picture with only spatial rather than temporal patterns. We introduced 3-dimensional CNN model [22], which has 3D convolution kernel and learns information not only from spatial but also temporal features by analysing the relationship between image sequences. In fact, 3D CNN has been used both in the classification task[23] and the regression task [24] in medical image detection with convincing performance achieved. We hope to make use of information from rhythmic pulse beating process as the typical temporal information at high resolution of 2048*1088.

The main contributions of this paper consist three parts: 1) We constructed wrist image dataset of our own, which contains near 500 different labels of TCM pulse localization. 2) We proposed an advanced way to construct model of 3DCNN by adding temporal rhythms, and to improve object localization accuracy. 3) We optimized the structure of the traditional CNN model by ablation experiments, and explained the effectiveness of this model from the perspective of model's visualization.

The rest of this paper is organized as follows: section 2 introduces our experiment works, include how we collect and pretreatment the data; Section 3 shows the method of model's construction; Section 4 reports the results based on the proposed 3DNIF model; Section 5 shows the discussion Section 6 shows the conclusion finally.

2 Methods

In order to improve the accuracy of palpation localization, we propose an advanced localization model based on 3D convolutional neural network and applied to infrared video of radial artery. The 3D convolution kernel is introduced to enrich model's ability to extract spatial and temporal features from circulatory pulsations. This can more accurately predict the location of the radial artery in the wrist.

2.1 Data Acquisition

In our research, in order to erase the interference from environmental light inference, the near infrared camera from HIKVISIONH MV-CA050-20GN was used for collecting high quality wrist video of volunteers' forearm (Fig.1). In this study, we recruited a total of 50 people to participate in data collection.

During experiment, the distance from camera to wrist was set to approximately the same, and the resolution of each video is 2048*1088. For each volunteer, any obvious bracelet in the wrist was asked for removal, and there was no scar on the wrist. 10 different inclination degree of forearm position were obtained, and each position was recorded for 8 seconds at 30 frames per second. Moreover, for each recording video, volunteer's radial artery location

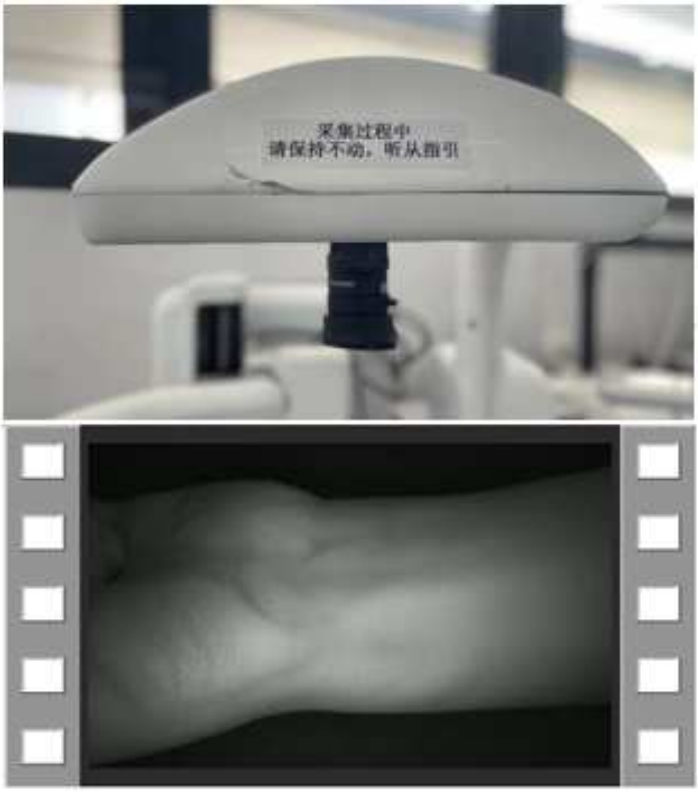

Fig. 1 The infrared camera from HIKVISIONH MV-CA050-20GN and the video type it collects.

was checked by the experimenter and presenting pixel was recorded. All procedures performed in studies involving human participants were in accordance with the ethical standards of the Ethics Committee of Fudan University School of Life Science and with the 1964 Helsinki declaration and its later amendments or comparable ethical standards.

2.2 Data Preprocessing

The frequency of the artery pulsation is 60-100Hz, which means it can contain at least 2 periods for each 2 seconds. To reduce the computation complex, we selected 2 seconds (60 frames) from each recording as the video for model training. Each pixel range from 0 to 255 at recording, and we use zero-mean normalization (z-score) to normalize pixels at each video frame. In this part, both frame reducing and normalizing can help to reducing over-fitting during the training period and reduce computational redundancy. Here shows the function of z-score(1), $\hat{x}$ is the mean value of input data, σ is the standard

deviation of input data.

$$z - score(x) = \frac{x - \hat{x}}{\sigma} \tag{1}$$

2.3 Design and setting of the Localization Networks

To increase the location accuracy by adding temporal information, 3D convolution kernels are presented at the convolutional feature map to extract features from local neighborhood. Therefore, the value of unit at each 2D CNN position(x,y) in the jth feature map in the ith layer[25], denoted as the function of(2), is added with one more dimension, and the value of each 3DCNN position(x,y,z) on the jth feature map in the ith layer is given by the function of (3). We employ the Mean Squared Error(MSE) loss for measurement of estimation differences (4):

$$v_{ij}^{xy} = tanh(b_{ij} + \sum_{m} \sum_{p=0}^{P_i-1} \sum_{q=0}^{Q_i-1} w_{ijm}^{pq} v_{(i-1)m}^{(x+p)(y+q)}) \tag{2}$$

$$v_{ij}^{xyz} = tanh(b_{ij} + \sum_{m} \sum_{p=0}^{P_i-1} \sum_{q=0}^{Q_i-1} \sum_{r=0}^{R_i-1} w_{ijm}^{pqr} v_{(i-1)m}^{(x+p)(y+q)(z+r)}) \tag{3}$$

$$Loss(MSE) = \sum_{i}^{N} (y_i - \hat{y}_i)^2 \tag{4}$$

$$f(x) = max(0, x) \tag{5}$$

We construct the model with the main structure as follows: input layer, convolutional layers (3D-conv), pooling layer, fully connected layer, and output layer (Fig.2). The proposed network contains 3 blocks and 2 fully connected layers, each block contains a 3D convolution layer and a pooling layer. As a kind of nonlinear down sampling, pooling layer can help model to lower dimension, removing redundant information, compressing features, simplifying network complexity. It greatly diminishes the number of parameters that need to be optimized. For each layer, activation function is selected as Rectified Linear Units (ReLU) (5) to introduce nonlinear calculating and increase the expressive ability of model.

The rest part of 3D CNN networks is Fully Connected layer (FC layer), whose activation function can be Relu normally. However, in our regression task, the information feature extraction is mainly concentrated in the convolution layer, so we hope to reduce the network redundancy and accelerate the network training by simplified fully connected layer. Compared with Relu, linear function can be faster and higher efficiency.

3D-Unet based on 3D convolution kernel is also introduced to compare to the proposed model. Through its unique U-shaped structure, the convolution results of each layer are sampled down, sampled up and connected. The output is a 2-dimensional graph, mapped to a two-dimensional matrix with the same

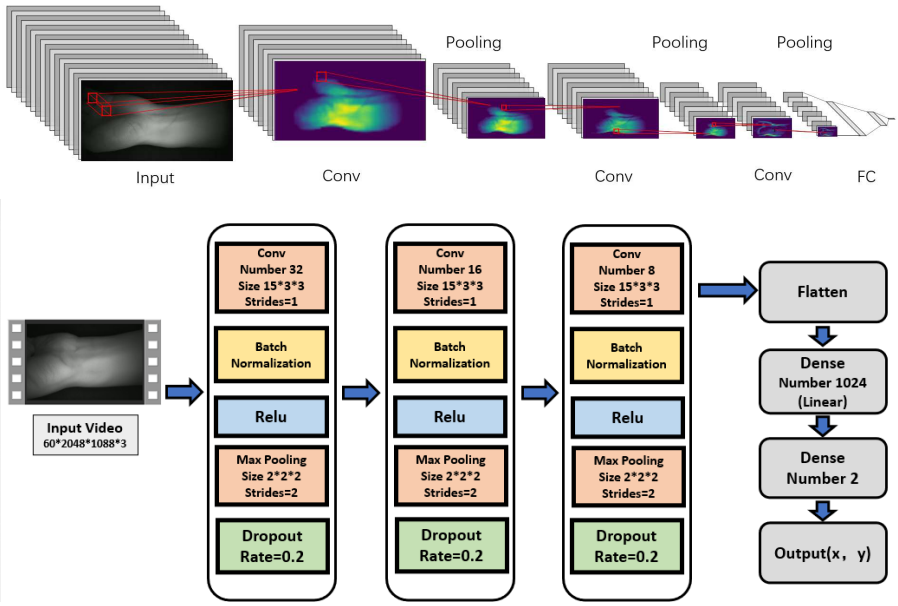

Fig. 2 The whole structure of this 3DCNN network. Our proposed method is to deal with input video by using 3D convolution kernel.

resolution as the input image. Then we extract the corresponding positioning coordinates from the output image as the final resulted coordinates. This model does not include a fully connected layer.

Finally, pixel distance is used as the evaluate metric, and the proportion of videos whose predicted distance from the label is less than the threshold is calculated as an evaluation index (7).

$$N_i = \{V_i, V_i[(y_i - \hat{y}_i)^2 <= T^2]\} \tag{6}$$

$$Accuracy = \frac{\mathrm{N}_i}{\mathrm{N}} * 100\% \tag{7}$$

y_i is the base truth of video V_i, $\hat{(y)}_i$ is the prediction of model, where we set threshold T, if $(\mathrm{y}_i - \hat{y}_i)^2 <= T^2$,$\mathrm{V}_i$ will belong to N_i which is the set of the videos whose prediction is considered as accurate. N is the set of valid videos. Threshold T will be set to 50,40,30,20.

3 Experiments

We have collected 500 videos from different people by infrared camera, each video was labeled by professional physicians with location of radial artery. Then 100 videos are chosen as valid set, the rest 400 video for training.

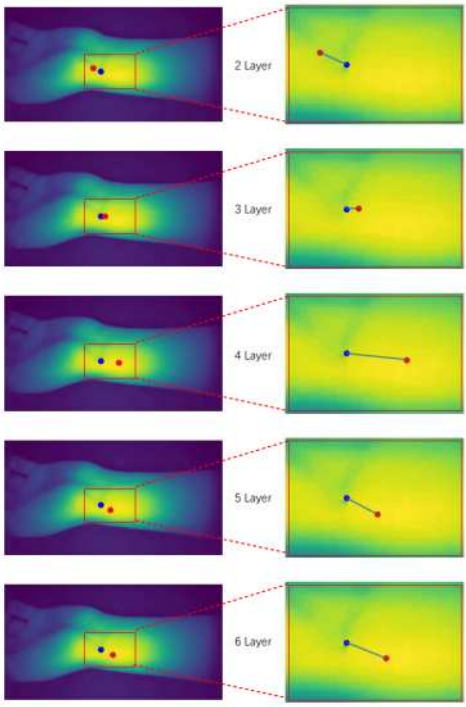

Fig. 3 The prediction performance from 3DCNN model with different hidden layers. Red point is the label pixel marked by experimenter, green point is prediction result

Table 1 Accuracy of 3DCNN in different number of filters

layers	Filters	50 pixel	40 pixel	30pixel	20 pixel
3	256	0.76	0.51	0.35	0.20
3	128	0.75	0.49	0.35	0.19
3	64	0.63	0.47	0.37	0.18
3	32	0.79	0.52	0.37	0.25
3	16	0.71	0.53	0.38	0.21

3.1 Ablation Study

Performance of the 3D CNN model is tested by adjusting different hyperparameters. First of all, we have tested the infulence of the number of convolutional layers (Fig. 3). The result show that best performance is shown when the layer number is selected as 3. We keep the layer number as 3, and adjust the number of filters by using the controlled variable method. Best performance and the accuracy are shown when filter is equal to 32 (Table 1). Then, we also control the layer number and the filter number, to test the influence of the size of convolution kernel filters. Results show that 15*3*3 and with dropout method are best according our experiment (Table 2).

Table 2 Accuracy of 3DCNN in different kernel size

kernel	50pixel	40pixel	30pixel	20pixel	Dropout
60*5*5	0.63	0.39	0.28	0.15	yes
60*3*3	0.79	0.52	0.37	0.25	yes
60*1*1	0.74	0.50	0.34	0.18	yes
30*3*3	0.75	0.54	0.38	0.17	yes
15*3*3	0.87	0.61	0.45	0.27	yes
15*3*3	0.81	0.56	0.34	0.22	no
8*3*3	0.78	0.59	0.31	0.20	yes

Table 3 Comparing with other classical networks

Threshold	AlexNet	Vgg16	Vgg19	3DCNN
50 pixels	72%	69%	74%	87%
40 pixels	57%	59%	57%	61%
30 pixels	37%	42%	35%	45%
20 pixels	15%	15%	18%	27%

3.2 Compare with 2D CNN

The extracted features from kernel convolution reflect information of the wrist radial artery. We visualised each layer processing results to recognize model effects. From left to right, they represent the output of first layer, second layer and third layer, 2DCNN has already reflected much information learned from the edge, contour, texture of the wrist. However, results are blurry, with the edge overlapped with background and the contour indistinct. Overall, the information of skin texture can be well reflected, but doesn't make the wrist artery and other parts obviously differentiated. We also tagged the relevant filtering result using red rectangles, shown as Fig.4(a). With limited number of red rectangles, result shows that 2DCNN can get limited useful information. For 3D CNN with added temporal information, result shows that the rhythmic pulsation presents at radial artery at wrist in a large portion of the filtered results, shown as (Fig4(b)). Information with low correlation with frequency was discarded reasonably, and this result helps to validate that 3D CNN can extract targeted rhythmic features better than 2DCNN.

After we apply both 2DCNN and 3DCNN models to fit for radial artery location at the wrist. Here is one example is as shown(Fig. 5), it shows that the distance from the 3DCNN prediction point to the target point is closer than the distance from the 2DCNN prediction point to the target point. Then, we had compared the euclidean distance between models results and target labeled point. It can be clearly seen from the figure that as the accuracy required for positioning gradually increases, 3DCNN model has obviously higher accuracy than the 2DCNN model.

3.3 Compare with 2D Classical Networks

Expect our earlier developed 2DCNN model, we also compare the proposed 3DCNN method with classical networks for object detection such as AlexNet, VGG16, and VGG19. Due to the input of these networks model requires small

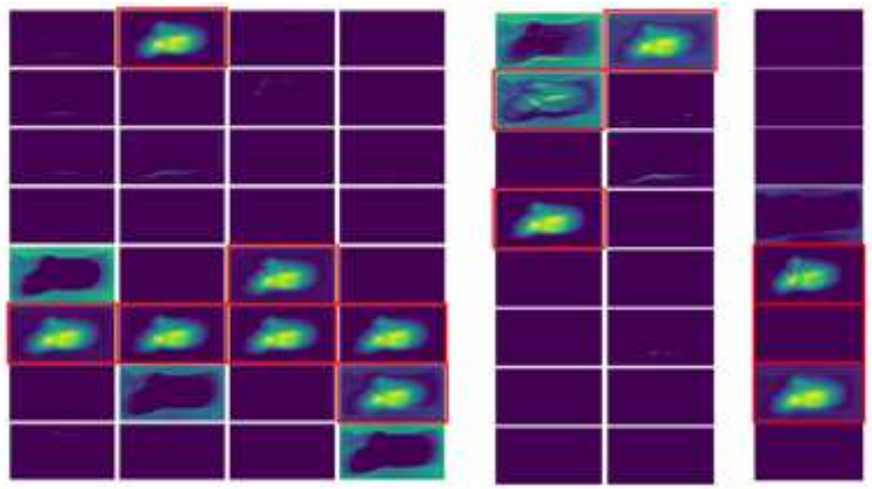

(a) The outputs of each convolutional layer from 2DCNN

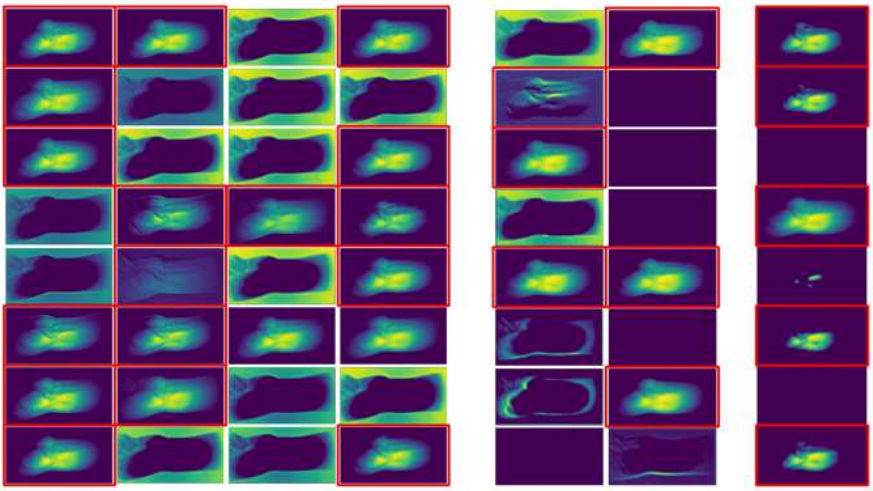

(b) The outputs of each convolutional layer from 3DCNN

Fig. 4 Outputs of each convolutional layer between 2DCNN model and 3DCNN model. From left to right, they represent the output of first layer, second layer and third layer. The light area demonstrates localised features that the model learned, and the red rectangles emphasize desired information detected at each convolutional layer.

size (224*224), we resize the images before feeding to networks for pulse localization. After the training, we expand the size proportionally to find detecting pixel locations. Results show that 3DCNN model outperformed other models in all distance thresholds, as Table 3 showing the localization examples and (Fig. 6) showing the pulse localization results comparison.

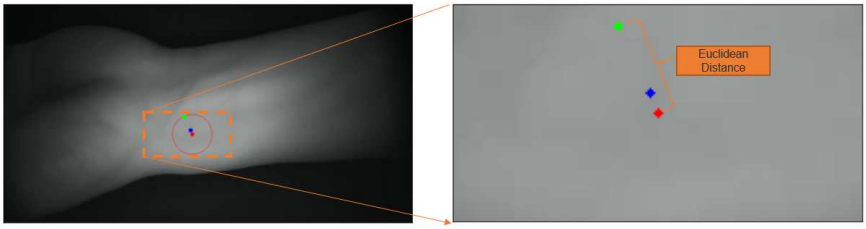

Fig. 5 The prediction performance between 2DCNN model and 3DCNN model. Red point is the label pixel marked by experimenter, green point is prediction results from 2DCNN, blue point is prediction results from 3DCNN.

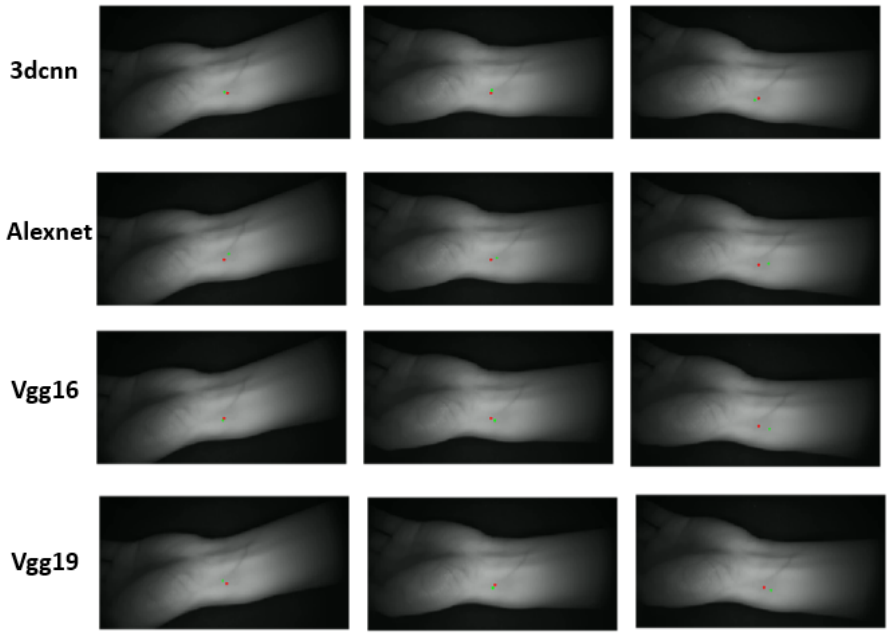

Fig. 6 The prediction performance of each 2D Classical Networks. Red point is the label pixel marked by experimenter, green point is prediction results from each model.

3.4 Compare with 3D-Unet Networks

To valid our model has unique performance, we introduce a 3D-Unet model with convolution Kernels set as same type as the proposed 3DCNN model. Results shows that 3D type model represented by both 3DCNN and 3D-Unet have better performance than 2D type model, shown as Fig. 7. In the case of same 3D convolutional, 3DCNN contains fully connected layers has higher accuracy in radial artery locating than 3D-Unet.

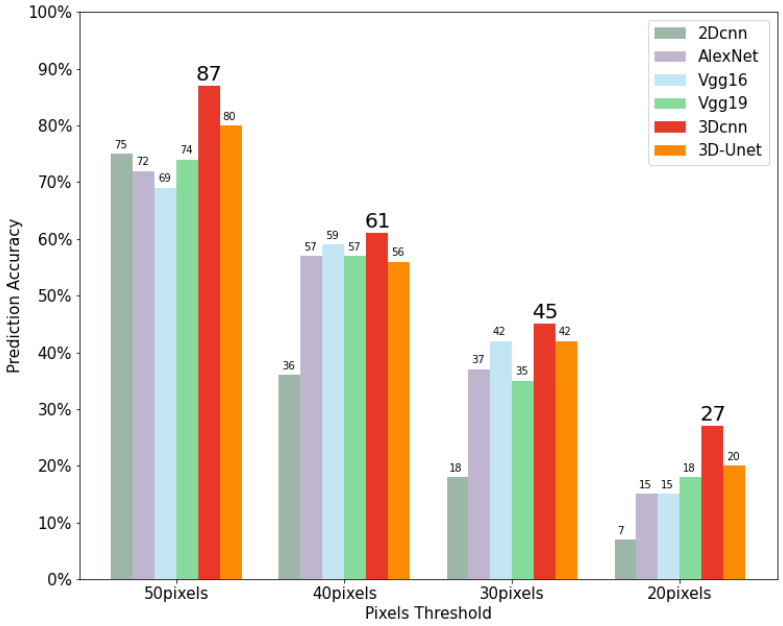

Fig. 7 Model comparison of 3DCNN with 3D-unet in different pixel distance.

4 Discussion

4.1 The Effection of Location

Palpation localization of radial artery is the foundation of pulse diagnosis which is an indispensable part of the principle 4-methods of diagnosis in Traditional Chinese Medicine. In this paper, We assess the effectiveness of 3DCNN on locating radial artery upon radius at the wrist by medical video data from infrared camera. The traditional 2DCNN locating model focuses on analyzing a single picture[26], by extracting spatial feature from convolutional layers, 2DCNN can learn relevant spatial information features such as wrist skin texture[27], therefore, for most standard groups, 2DCNN can achieve nice localization results. However, from an anatomical point of view, the interlaced meridians of the body's wrists are complicated[28]. The relative position between the radial artery and the radius does not have a clear distance range in space, such as Oblique flying pulse[29].In this special situation, the 2DCNN, which can only learn spatial information, shows its original limitations[18]. In order to solve the problem of inaccurate positioning caused by insufficient information extraction in 2DCNN, we increase the temporal and spatial information by introducing a 3D convolution kernel The results

show the comparison between the positioning prediction effect of 3DCNN and 2DCNN. In order to increase the credibility of the results, we also added four additional sets of comparative experiments, including three classic models, AlexNet[30],Vgg16[31],Vgg19[32], which have 2d convolution kernel structure and 3D-Unet[33] that also has 3d convolution kernel structure. The result shows that our proposed 3DCNN model on task of locating with improvements of 20%, 12%,12%,9%,7% on 20pixels than 2DCNN,AlexNet,Vgg16,Vgg19,3D-Unet, respectively. An improvement of 20% and 7% is achieved better than 2DCNN and 3D-Unet is significant. Because, in addition to 3D convolution kernel, 2DCNN and 3DCNN are very similar in networks structure. Both 3D-Unet and 3DCNN have 3D convolution kernel, but 3D-Unet has more complex U-shaped network structure than 3DCNN, thereby it becomes a challenging task to adjust the complexity of our model with in 3D convolution kernel.Even in this rare case, we find that 3DCNN can provide more visually accurate results. Therefore, we believe that our proposed architecture can serve as a viable location tool for palpation localization of radial artery.

4.2 The Limitation of This Study and Further work

There is limitation in our study in this work. Fist of all, there was only 50 young people with 500 videos are used to train and verify the accuracy of the system, all of them in the same age range at middle twenties. With the age increasing, the human collagen will be losing, the skin becomes loose and the pulsation of the wrist becomes emerge, so the radial artery position of the wrist of the elderly is more easily detected[34], so it is not considered. And all this test sample has standard BMI, and with high BMI subject, the skin will be thicker[35], pulse beats information is getting difficult to be captured by camera, incomplete training samples will greatly reduce the universality of the model. Meanwhile, the detection accuracy of the system is affected by the accuracy of the infrared camera[36] itself which including photosensitive components, lens quality, color depth,. However, the higher the accuracy, the higher the price of the infrared camera itself. In addition, on the algorithm we have just discussed the difference between 3DCNN and 3D-Unet, the comparison model which contains 3D convolution kernel seems inadequate. At the same time, limited by the memory of the original computer, when we compared the effects of different neurons and neural network layers of 3DCNN on the final result, we only performed a partial comparison. If you increase the size of the data set, perhaps a deeper network structure can build a better prediction model

In the future work, We will expand the dimension of the data set, so that the training data of the model can cover more widely in terms of age, BMI and gender. At the same time, we will increase budget in order to adopt more precise and better quality near-infrared cameras to collect data. The last but not least, we will further optimize the positioning algorithm, on the basis of 3D structure, deep exploring the network structure of this model. In addition, other algorithms with the same 3D structure beside 3d-Unet Will be included

in the comparative experiment,and the results will be reported promptly in the near future.

5 Conclusion

In this paper, a new approach of using 3DCNN networks was explored to automatically and accurately find radial artery from wrist video. The core idea is to convolve the input image sequence by 3D convolution kernel .This proposed model makes full use of the abundant temporal information contained in radial artery pulsation. The ablation study shows that best performance at network structure of layer number as 3, the size of kernel as 15*3*3. For different distance threshold setup, our model performs with accuracy as 0.87 at 50 pixels, accuracy as 0.61 at 40 pixels, accuracy as 0.45 at 30 pixels, accuracy as 0.27 at 20 pixels, when resolution are 2048*1088. Meanwhile, this paper shows the advantages of 3DCNN not only from the results, but also in the principle of filtering process. In addition, we showed that 3DCNN can be easily scaled for improved performance.In the future, we will continue this research work by collecting further labeled videos to improve and increase the model robustness and trying to fuse models to improve the accuracy and precision. By extending this research, the authors wish to achieve a valuable impact on development of Traditional Chinese Medicine.

List of abbreviations

TCM:Traditional Chinese Medicine; 2DCNN:2-Dimensional Convolutional Neural Networks; 3DCNN:3-Dimensional Convolutional Neural Networks; CNN:Convolutional Neural Networks; FC layer:Fully Connected layer; ReLU:Rectified Linear Units; MSE:Mean Squared Error; VGG16:Visual Geometry Group Network 16; VGG19:Visual Geometry Group Network 19; AlexNet:Alex ImageNet;

Declarations

Availability of data and materials. Some data can be shared on request.

Competing interests. The authors declare no conflict of interest.

Funding. We thank the Key Area Support Plan of Guangdong Province for Jihua Laboratory (X190051TB190), Shanghai Municipal Science and Technology Major Project (2017SHZDZX01), Special projects in key fields of Guangdong Universities (next generation of information technology)(2020ZDZX3003) for supporting this work.

Authors' contributions. Conceptualization, Qiliang Chen and Jingjing Luo; Methodology, Jingjing Luo; Software, Yulin Huang; Validation, Qiliang Chen and Yulin Huang. and Zhongzhi Ji; Formal analysis, Qiliang Chen; Investigation, Qiliang Chen; Resources, Qiliang Chen.; Data curation, Zhongzhi

Ji; Writing—original draft preparation, Qiliang Chen; Writing—review and editing, Qiliang Chen; Visualization, Xing Zhu.; Supervision, Qiliang Chen; Project administration, Jingjing Luo.; Funding acquisition, Jingjing Luo.

Acknowledgements. Authors acknowledge technical support from our institutional research teams.

References

[1] Rosemarie, Velik: An objective review of the technological developments for radial pulse diagnosis in traditional chinese medicine. European Journal of Integrative Medicine **7**(4), 321–331 (2015)

[2] Ko, M.M., Lee, M.S., Birch, S., Lee, J.A.: The reliability and validity of instruments measuring pattern identification in korean medicine: A systematic review. European Journal of Integrative Medicine **15**, 47–63 (2017)

[3] Geng, X., Liu, S., Zhang, Y., Hou, J., Zhang, H.: A noncontact method for locating radial artery above radial styloid process in thermal image. Evidence-based Complementary and Alternative Medicine **2020**(2), 1–9 (2020)

[4] Wang, H., Cheng, Y.: A quantitative system for pulse diagnosis in traditional chinese medicine. In: 2005 IEEE Engineering in Medicine and Biology 27th Annual Conference (2006)

[5] Nanyue, W., Youhua, Y., Yan, C., Zengyu, S., Tongda, L., Yanping, C.: Research of length of cun,guan and chi in pulse taking. China Journal of Traditional Chinese Medicine Pharmacy (2009)

[6] Yan-Ping, L., Cen-Han, H.: Traditional and modern research of 'taking pulse at cunkou alone' method. China Journal of Traditional Chinese Medicine and Pharmacy (2011)

[7] Wang, P., Zuo, W., Zhang, D.: A compound pressure signal acquisition system for multichannel wrist pulse signal analysis. IEEE Transactions on Instrumentation and Measurement **63**(6), 1556–1565 (2014)

[8] Wang, D., Zhang, D., Lu, G.: A novel multichannel wrist pulse system with different sensor arrays. IEEE Transactions on Instrumentation Measurement **64**(7), 2020–2034 (2015)

[9] Chung, Y.F., Hu, C.S., Luo, C.H., Yeh, C.C., Si, X.C., Feng, D.H., Yeh, S.M., Liang, C.H.: Possibility of quantifying tcm finger-reading sensations: Ii. an example of health standardization. European Journal of Integrative Medicine **4**(3) (2012)

[10] Hu, C.S., Chung, Y.F., Yeh, C.C., Luo, C.H.: Temporal and spatial properties of arterial pulsation measurement using pressure sensor array. Evidence-based complementary and alternative medicine : eCAM **2012**(1741-427X), 745127–745127 (2012)

[11] Bae, J.H., Jeon, Y.J., Kim, J.Y., Kim, J.U.: New assessment model of pulse depth based on sensor displacement in pulse diagnostic devices. Evidence-Based Complementray and Alternative Medicine,2013,(2013-9-25) **2013**(1), 938641 (2013)

[12] Nevatia, R.: Locating object boundaries in textured environments. IEEE Transactions on Computers **C-25**(11), 1170–1175 (1976)

[13] Jiang, H., Fan, X.Y.: Centroid locating for star image object by fpga. Advanced Materials Research **403-408**, 1379–1383 (2011)

[14] Denman, S., Halstead, M., Fookes, C., Sridharan, S.: Locating people in surveillance video using soft biometric traits (2017)

[15] Ennio, G., Angela, A., Alberto, B., Laura, B., Enea, C., Sandro, F., Paola, P., Manola, R., Agnese, S., Susanna, S.: Heart rate detection using microsoft kinect: Validation and comparison to wearable devices. Sensors **17**(8), 1776 (2017)

[16] Fang, L.Y., Christopher, V., Charles, W.P., Ray, P.N., Christian, I.J., Andrade, F.P.A., Choon-Sung, L.S.: Noninvasive free flap monitoring using eulerian video magnification. Case Reports in Otolaryngology,2016,(2016-3-22) **2016**, 1–4 (2016)

[17] Jason, Adleberg, Ashley, P, O'Connell, Ferster, Daniel, A, Benito, and, R.: Detection of muscle tension dysphonia using eulerian video magnification: A pilot study. Journal of Voice Official Journal of the Voice Foundation (2019)

[18] LUO, J., CHUN, O., NIE, X., YIN, W., LU, H., GUO, Y.: Accurate targeting in robot-assisted tcm pulse diagnosis using adaptive sensor fusion. Periodicals of Engineering and Natural Sciences **7**(1), 381–387 (2019)

[19] Yang, B., Meng, K., Lu, H., Nie, X., Huang, G., Luo, J., Zhu, X.: Pulse localization networks with infrared camera. In: ACM International Conference on Multimedia in Asia (2020)

[20] Krizhevsky, A., Sutskever, I., Hinton, G.: Imagenet classification with deep convolutional neural networks. In: NIPS (2012)

[21] Armato, S.G., Petrick, N.A., Thomaz, R.L., Carneiro, P.C., Patrocinio, A.C.: Feature extraction using convolutional neural network for classifying

breast density in mammographic images **10134**, 101342 (2017)

[22] Hara, K., Kataoka, H., Satoh, Y.: Can spatiotemporal 3d cnns retrace the history of 2d cnns and imagenet? In: CVPR2018 (2018)

[23] Li, Y., Tian, Y., Ge, B.: Lung cancer classification using 3d-cnn with a scheduled learning strategy. In: 2018 2nd International Conference on Artificial Intelligence: Technologies and Applications (ICAITA 2018) (2018)

[24] Liyuan, Chen, Zhiguo, Zhou, David, Sher, Qiongwen, Zhang, Jennifer, and, S.: Combining many-objective radiomics and 3d convolutional neural network through evidential reasoning to predict lymph node metastasis in head and neck cancer. Physics in medicine and biology (2019)

[25] Ji, S., Xu, W., Yang, M., Yu, K.: 3d convolutional neural networks for human action recognition. IEEE Transactions on Pattern Analysis Machine Intelligence **35**(1), 221–231 (2013)

[26] Konstantinova, J., Jiang, A., Althoefer, K., Dasgupta, P., Nanayakkara, T.: Implementation of tactile sensing for palpation in robot-assisted minimally invasive surgery: A review. Sensors Journal, IEEE **14**(8), 2490–2501 (2014)

[27] Yu, J., Yang, B., Wang, J., Leader, J., Pu, J.: 2d cnn versus 3d cnn for false-positive reduction in lung cancer screening. Journal of Medical Imaging **7**(5) (2020)

[28] Terslev, L., Torp-Pedersen, S., Bang, N., Koenig, M.J., Bliddal, H.: Doppler ultrasound findings in healthy wrists and finger joints before and after use of two different contrast agents. Annals of the Rheumatic Diseases **64**(6), 824–827 (2005)

[29] Saint-Cyr, M., Mujadzic, M., Wong, C., Hatef, D., Lajoie, A.S., Rohrich, R.J.: The radial artery pedicle perforator flap: vascular analysis and clinical implications. Plastic Reconstructive Surgery **125**(5), 1469–78 (2010)

[30] Yuan, Z.W., Zhang, J.: Feature extraction and image retrieval based on alexnet. In: Eighth International Conference on Digital Image Processing (ICDIP 2016) (2016)

[31] Liu, B., Zhang, X., Gao, Z., Li, C.: Weld defect images classification with vgg16-based neural network. Springer, Singapore (2017)

[32] Bermeitinger, B., Donig, S., Christoforaki, M., Freitas, A., Handschuh, S.: Vgg19 (2017)

[33] Xiao, Z., Liu, B., Geng, L., Zhang, F., Liu, Y.: Segmentation of lung nodules using improved 3d-unet neural network. Symmetry **12**(11), 1787 (2020)

[34] Bailey, A.J., Sims, T.J., Ebbesen, E.N., Mansell, J.P., Thomsen, J.S., Mosekilde, L.: Age-related changes in the biochemical properties of human cancellous bone collagen: Relationship to bone strength. Calcified Tissue International **65**(3), 203–210 (1999)

[35] Falcone, M., Preto, M., Timpano, M., Ciclamini, D., Gontero, P.: The surgical outcomes of radial artery forearm free-flap phalloplasty in transgender men: single-centre experience and systematic review of the current literature. International Journal of Impotence Research, 1–9 (2021)

[36] Murphy, E.K.: Use of an infrared camera to improve the outcome of facial nerve monitoring. American journal of electroneurodiagnostic technology **48**(1), 38–47 (2008)